Controller Synthesis for String Stability of Vehicle Platoons

Jeroen Ploeg, Dipan P. Shukla, Nathan van de Wouw, and Henk Nijmeijer, *Fellow, IEEE*

***Abstract*—Cooperative adaptive cruise control (CACC) allows for short-distance automatic vehicle following using intervehicle wireless communication in addition to onboard sensors, thereby potentially improving road throughput. In order to fulfill performance, safety, and comfort requirements, a CACC-equipped vehicle platoon should be string stable, attenuating the effect of disturbances along the vehicle string. Therefore, a controller design method is developed that allows for explicit inclusion of the string stability requirement in the controller synthesis specifications. To this end, the notion of string stability is introduced first, and conditions for $\mathcal{L}_2$ string stability of linear systems are presented that motivate the development of an $\mathcal{H}_\infty$ controller synthesis approach for string stability. The potential of this approach is illustrated by its application to the design of controllers for CACC for one- and two-vehicle look-ahead communication topologies. As a result, $\mathcal{L}_2$ string-stable platooning strategies are obtained in both cases, also revealing that the two-vehicle look-ahead topology is particularly effective at a larger communication delay. Finally, the results are experimentally validated using a platoon of three passenger vehicles, illustrating the practical feasibility of this approach.**

***Index Terms*—Cascaded systems, cooperative adaptive cruise control (CACC), string stability, vehicle platoons, $\mathcal{H}_\infty$ optimal control.**

I. Introduction

COOPERATIVE adaptive cruise control (CACC) can be regarded as an extension of the adaptive cruise control (ACC) functionality. ACC is a vehicle-following control system that automatically accelerates and decelerates a vehicle to keep a desired distance to the preceding vehicle and, in the absence of one, aims for a constant cruise speed [1]. The intervehicle distance and its rate of change are commonly measured by a radar. A CACC system arises when ACC is extended with wireless intervehicle communications [2]. This enables vehicles to obtain information beyond the line-of-sight of onboard sensors and to obtain information of other vehicles that cannot be retrieved otherwise. As a result, short intervehicle distances can be realized, thus increasing traffic throughput, without compromising safety [3]. In addition, significant fuel savings are possible, particularly for trucks [4].

The vehicle-following objective, which is essential to CACC, is subject to requirements related to safety, comfort, and scalability with respect to platoon length. In order to fulfil these requirements, the vehicle platoon is desired to exhibit string-stable behavior [5], which can be loosely characterized as the attenuation of the effects of disturbances along the platoon. Typical disturbances are, e.g., velocity variations of the lead vehicle or initial condition perturbations of the platoon vehicles.

Various types of controllers that realize string-stable behavior have been proposed in the literature; see, e.g., [6] for a proportional-derivative-like controller and [7], describing a sliding-mode controller. These controller synthesis methods, however, do not allow taking the string stability requirement explicitly into account. Consequently, string-stable behavior has to be realized through *a posteriori* controller tuning. Due to its capability of including constraints in the controller design, the application of model predictive control for vehicle platooning also received quite some attention. As a relevant example, [8] proposes a controller employing a one-vehicle look-ahead communication topology, with the attenuation of the $\mathcal{L}_\infty$ norm of the disturbance responses as a constraint. In [9], an $\mathcal{H}_\infty$ optimal platoon controller is synthesized, also using a one-vehicle look-ahead topology, which focuses on the effect of packet loss on performance in terms of disturbance attenuation, thus being very closely related to string stability. A mixed $\mathcal{H}_2/\mathcal{H}_\infty$ problem formulation is applied in [10], with string stability as one of the optimization criteria for controller synthesis, resulting in a centralized controller that requires the states of all platoon vehicles to be available.

Due to its relevance for application in everyday traffic, this paper focuses on ad hoc vehicle platooning, i.e., a decentralized solution without a designated platoon leader (as opposed to [10]), aiming to develop a systematic controller design method in which the string stability requirement is *a priori* included as a design specification. To this end, $\mathcal{H}_\infty$ optimal controller synthesis is applied, since this approach appears to naturally fit the $\mathcal{L}_2$ string stability conditions for linear cascaded systems, among which vehicle platoon models. In addition, $\mathcal{H}_\infty$ control allows to explicitly make tradeoffs between vehicle-following performance and string stability. It is illustrated through controller synthesis for one- and two-vehicle look-ahead schemes that the controller design method supports the generic n-vehicle look-ahead communication topology, extending the one-vehicle look-ahead approaches in [8] and [9]. Finally, the practical feasibility of the controllers is shown through experimental evaluation in a platoon of three passenger vehicles.

Manuscript received May 31, 2013; revised August 25, 2013 and November 4, 2013; accepted November 13, 2013. Date of publication December 12, 2013; date of current version March 28, 2014. The Associate Editor for this paper was M. Da Lio.

J. Ploeg is with the Integrated Vehicle Safety Department, TNO, 5700 AT Helmond, The Netherlands (e-mail: jeroen.ploeg@tno.nl).

D. P. Shukla is with Continental Reifen Deutschland GmbH, 30165 Hannover, Germany (e-mail: dipan.paresh.shukla@conti.de).

N. van de Wouw and H. Nijmeijer are with the Department of Mechanical Engineering, Eindhoven University of Technology, 5612 AZ Eindhoven, The Netherlands (e-mail: n.v.d.wouw@tue.nl; h.nijmeijer@tue.nl).

Color versions of one or more of the figures in this paper are available online at http://ieeexplore.ieee.org.

Digital Object Identifier 10.1109/TITS.2013.2291493

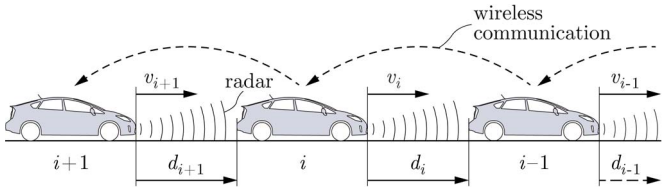

Fig. 1. CACC-equipped homogeneous vehicle platoon.

The outline of this paper is as follows: Section II formulates the control problem and derives a platoon model that forms the basis for the controller synthesis approach. Section III introduces the notion of $\mathcal{L}_2$ string stability and presents string stability conditions for linear systems, upon which Section IV casts the control problem into the $\mathcal{H}_\infty$ framework. The actual controller synthesis is performed in Section V, and the experimental results obtained with the designed controllers are presented in Section VI. Section VII summarizes the main conclusions.

II. Control Problem Formulation

Consider a homogeneous platoon of m vehicles, as depicted in Fig. 1, where d_i is the distance between vehicle i and its preceding vehicle $i-1$, and v_i is the velocity of vehicle i. The main objective of each vehicle in the platoon (except the lead vehicle) is to follow its preceding vehicle at a desired distance $d_{r,i}$. Adopting the constant time headway spacing policy, which is known to improve string stability [6], [11], the desired distance reads

$$d_{r,i}(t) = r_i + hv_i(t), \qquad i \in S_m \backslash \{1\} \tag{1}$$

where h is the time headway, and r_i is the standstill distance. In (1), $S_m = \{i \in \mathbb{N} \mid 1 \leq i \leq m\}$ is the set of all vehicles in a platoon of length $m \in \mathbb{N}$. This paper focuses on homogeneous platoons, which is why h does not depend on the vehicle index. The spacing error $e_i(t)$ is then equal to

$$\begin{aligned} e_i(t) &= d_i(t) - d_{r,i}(t) \\ &= (q_{i-1}(t) - q_i(t) - L_i) - (r_i + hv_i(t)) \end{aligned} \tag{2}$$

where q_i is the rear-bumper position of vehicle i, and L_i is its length. The platoon control problem is now twofold. First, the platoon is subject to the vehicle-following objective, i.e.,

$$a_1(t) = 0 \,\forall\, t \geq 0 \Rightarrow \lim_{t\to\infty} e_i(t) = 0 \,\forall\, i \in S_m \backslash \{1\} \tag{3}$$

where a_1 is the acceleration of the lead vehicle; in other words, with the first vehicle driving at a constant velocity, the spacing errors e_i should converge to zero. Second, the string stability requirement is imposed, as described in Section III.

Adopting the platoon model as employed in [12] and [13], the vehicle dynamics are described in the Laplace domain by the transfer function $G(s)$, with $s \in \mathbb{C}$, according to

$$G(s) = \frac{q_i(s)}{u_i(s)} = \frac{1}{s^2(\tau s + 1)} e^{-\phi s} \tag{4}$$

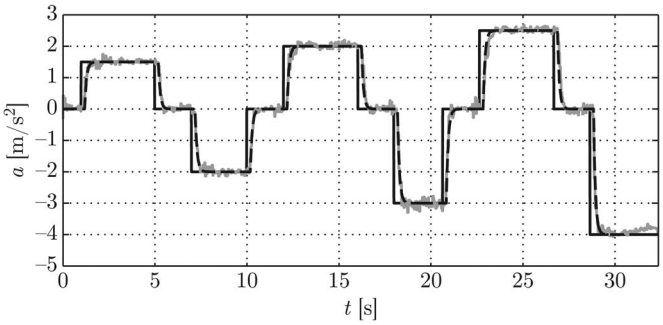

Fig. 2. Step response of an acceleration-controlled test vehicle: desired acceleration (solid black), measured acceleration (gray), and simulated acceleration (dashed black).

where τ is a time constant, and ϕ is a time delay. u_i is the vehicle input (desired acceleration), whereas the position q_i is the output. Note that $\cdot(s)$ denotes the Laplace transform of the corresponding time-domain variable $\cdot(t)$; if the argument is omitted, then the domain is either irrelevant or can be easily devised from the context. Due to the homogeneity assumption, $G(s)$ is identical for all vehicles. Despite its simplicity, $G(s)$ adequately describes the dynamics of the native force-controlled hybrid driveline of the test vehicles (see Section VI), including a precompensator to convert the desired acceleration to the desired force, taking into account the actual vehicle mass and the estimated drag forces. This is confirmed in Fig. 2, which shows the desired acceleration, the measured acceleration response, and the simulated response of the model $G_a(s) = 1/(\tau s + 1)e^{-\phi s}$, with $\tau = 0.1$ s and $\phi = 0.2$ s. Obviously, this model does not hold for limit situations, such as emergency braking, which are characterized by nonlinear behavior due to tire slip and complex braking system dynamics. Such limit situations, however, are considered to be outside the operational range of CACC.

Formulating the spacing error $e_i(t)$ in (2) in the Laplace domain yields

$$e_i(s) = q_{i-1}(s) - H(s)q_i(s) \tag{5}$$

with the spacing policy transfer function $H(s)$ defined as

$$H(s) = hs + 1. \tag{6}$$

Without loss of generality, $r_i = L_i = 0$ is assumed in the remainder of this paper. Inspired by [12], the structure of the controller of each vehicle is chosen according to

$$\begin{aligned} u_i(s) &= H^{-1}(s) \left(K_{\mathrm{fb}}(s) e_i(s) + \sum_{j=1}^{k} K_{\mathrm{ff},j}(s) u^*_{i-j}(s) \right) \\ &= H^{-1}(s) K(s) \begin{pmatrix} e_i(s) \\ u^*_{i-1}(s) \\ \vdots \\ u^*_{i-k}(s) \end{pmatrix} := H^{-1}(s) \xi_i(s) \end{aligned} \tag{7}$$

where $K_{\mathrm{fb}}(s)$ represents the feedback control law; $K_{\mathrm{ff},j}(s)$, $j = 1, 2, \ldots, k$, represents the feedforward controllers, and

$K(s) = (K_{\text{fb}}(s)\ K_{\text{ff},1}(s)\ \ldots\ K_{\text{ff},k}(s))$. $\xi_i(s)$ is the output of the controller $K(s)$. Note that the precompensator $H^{-1}(s)$ in (7) cancels the spacing policy transfer function $H(s)$, which is located in the feedback loop according to (5), such that the driver can select any time headway h without compromising individual vehicle stability. Due to the ad hoc platooning concept, $K(s)$ is desired to be independent of the vehicle index i. u_{i-j}^*, $j = 1, 2, \ldots, k$, are the inputs of k preceding vehicles, which are obtained through wireless intervehicle communication with a latency θ, i.e., $u_{i-j}^*(t) = u_{i-j}(t-\theta)$. In the Laplace domain, this latency is modeled by a transfer function $D(s) = e^{-\theta s}$, being (approximately) the same for all preceding vehicles because all vehicles broadcast their information. It should be mentioned that the usage of wireless communication introduces time-varying sampling intervals, which may be relevant to the string stability characteristics [14]. Assuming a sufficiently high sampling frequency of the discrete-time controller implementation, these sampled-data effects are ignored here.

The controller (7) is thus required to realize asymptotic tracking of the preceding vehicle according to (3), under the additional requirement of string stability, with the latter being formally introduced in the next section.

III. String Stability

A comprehensive overview of the various interpretations of string stability that exist in the literature is given in [13], based on which a novel definition for $\mathcal{L}_p$ string stability was introduced. Here, this definition is extended to better support a multiple-vehicle look-ahead CACC design. In doing so, we focus on $\mathcal{L}_2$ string stability for linear systems since the controller synthesis to be developed in Section V will specifically support this type of string stability and the vehicular platooning models in Section II are linear. Consider to this end the cascaded state-space system, with $i \in S_m$,

$$\begin{aligned} \dot{x}_i &= \sum_{j=1}^{i} A_{i-j} x_j + B_{i-1} u_1 \\ y_i &= C x_i \end{aligned} \tag{8}$$

representing a homogeneous system with a unidirectional interconnection topology. A_k and B_k $(k = 0, 1, \ldots, m-1)$ are the system and input matrices, respectively, and C is the output matrix. $u_1 \in \mathbb{R}^\ell$ is the external input, and $x_i \in \mathbb{R}^n$ and $y_i \in \mathbb{R}^\ell$, $i \in S_m$ are the state and the output, respectively. Note that, in view of the upcoming string stability conditions, the system is assumed to be square, having ℓ inputs and outputs. In case (8) represents a controlled vehicle platoon, the state may be defined as $x_i^T = (e_i\ v_i\ a_i\ \ldots)$, where e_i is the distance error, v_i is the vehicle velocity, and a_i is the vehicle acceleration, whereas additional states may be present due to controller dynamics. With $u_1 \equiv 0$, the system (8) may then have constant equilibrium states $\bar{x}_i^T = (0\ \bar{v}_1\ 0\ \ldots)\ \forall i \in S_m$, where $\bar{v}_1$ is a constant lead vehicle velocity. This can be readily understood, since the string would be in equilibrium when all vehicles drive at the same constant speed with zero spacing error. Introducing the lumped state vector $x^T = (x_1^T\ x_2^T\ \ldots\ x_m^T)$, (8) can be reformulated as

$$\begin{aligned} \dot{x} &= Ax + Bu_1 \\ y_i &= C_i x, \qquad i \in S_m \end{aligned} \tag{9}$$

where A is a lower block-triangular matrix, with the matrices A_0 on the main diagonal, the matrices A_1 on the subdiagonal, etc. Furthermore, $B^T = (B_0^T\ B_1^T\ \ldots\ B_{m-1}^T)$, and $C_i = (0_{\ell \times n(i-1)}\ C\ 0_{\ell \times n(m-i)})$. String stability can now be defined as follows.

Definition 1 ($\mathcal{L}_2$ String Stability): The system (9), with a constant equilibrium solution $\bar{x}$ for $u_1 \equiv 0$, is $\mathcal{L}_2$ *string stable* if there exist class $\mathcal{K}$ functions[1] α and β, such that, for any initial state $x(0) \in \mathbb{R}^{mn}$ and any $u_1 \in \mathcal{L}_2^\ell$, it holds that

$$\|y_i(t) - C_i\bar{x}\|_{\mathcal{L}_2} \le \alpha\left(\|u_1(t)\|_{\mathcal{L}_2}\right) + \beta\left(\|x(0) - \bar{x}\|\right) \quad \forall\, i \in S_m \text{ and } \forall\, m \in \mathbb{N}. \tag{10}$$

If, in addition to (10), with $x(0) = \bar{x}$ it also holds that

$$\|y_i(t) - C_i\bar{x}\|_{\mathcal{L}_2} \le \|y_1(t) - C_1\bar{x}\|_{\mathcal{L}_2} \quad \forall\, i \in S_m\backslash\{1\} \text{ and } \forall\, m \in \mathbb{N}\backslash\{1\} \tag{11}$$

the system (9) is *semi-strictly $\mathcal{L}_2$ string stable* with respect to its input u_1. If, in addition to (10), with $x(0) = \bar{x}$ it also holds that

$$\|y_i(t) - C_i\bar{x}\|_{\mathcal{L}_2} \le \|y_{i-1}(t) - C_{i-1}\bar{x}\|_{\mathcal{L}_2} \quad \forall\, i \in S_m\backslash\{1\} \text{ and } \forall\, m \in \mathbb{N}\backslash\{1\} \tag{12}$$

the system (9) is referred to as *strictly $\mathcal{L}_2$ string stable* with respect to its input u_1.

Here, $\|\cdot\|$ denotes any vector norm, $\|\cdot\|_{\mathcal{L}_2}$ denotes the signal 2-norm [15], and $\mathcal{L}_2^\ell$ is the ℓ-dimensional space of vector signals that are bounded in the $\mathcal{L}_2$ sense. It is noted that Definition 1 closely resembles the common $\mathcal{L}_2$ stability definition [16] as far as (nonstrict) $\mathcal{L}_2$ string stability is concerned, except for the fact that the inequality (10) must hold *for all* string lengths $m \in \mathbb{N}$.

The notion of (semi-)strict $\mathcal{L}_p$ string stability, for which not only (10) must hold but also (11) or (12), has been introduced to accommodate the requirement of upstream disturbance attenuation, as already mentioned in Section I. Compared to [13], the novel notion of semi-strict string stability has been introduced here to support the controller design in the two-vehicle look-ahead scheme, as will become clear in Section V.

It is noted that the system with index $i = 1$ may be either uncontrolled or, in case of vehicle platoons, velocity controlled. Alternatively, it is also possible to apply a vehicle-following controller with a so-called virtual reference vehicle. Choosing u_1 as the external platoon input encompasses all such options, thus yielding the most generic approach.

[1] A continuous function $\alpha : [0, a) \mapsto [0, \infty)$ is said to belong to class $\mathcal{K}$ if it is strictly increasing and $\alpha(0) = 0$.

Definition 1 provides a basis for easy-to-check string stability conditions. To this end, the model (9) is first formulated in the Laplace domain as follows:

$$y_i(s) = P_i(s)u_1(s) + O_i(s)x(0), \qquad i \in S_m \tag{13}$$

with $x(0)$ denoting the initial (time-domain) condition, and $P_i(s) = C_i(sI - A)^{-1}B$ and $O_i(s) = C_i(sI - A)^{-1}$. Because the system with index $i = 1$ is assumed to be uncontrolled, (9) may contain unstable and/or marginally stable modes. Consequently, $P_i(s)$ may be unstable, leading to the following assumption.

Assumption 1: The output y_i, $i \in S_m$, is chosen such that unstable and marginally stable modes of the system (9) are unobservable.

As a consequence of Assumption 1, it holds that, for linear time-invariant systems, if the function α in (10) exists, then also the function β exists. In view of string stability, it therefore suffices to only analyze the input–output behavior, characterized by $P_i(s)$, which is equivalent to assuming $x(0) = \bar{x}$ in (13). To simplify the synthesis of string stability conditions, $\bar{x} = 0$ is chosen without loss of generality, since there always exists a coordinate transformation yielding the origin as the equilibrium.

Provided that $P_i(s)$ represents a causal and stable system, its $\mathcal{H}_\infty$ norm $\|P_i(s)\|_{\mathcal{H}_\infty}$ is defined as

$$\|P_i(s)\|_{\mathcal{H}_\infty} := \sup_{Re(s)>0} \bar{\sigma}\left(P_i(s)\right) \tag{14}$$

where $\bar{\sigma}(\cdot)$ denotes the maximum singular value.[2] It can be then shown [15, p. 101] that $\|P_i(s)\|_{\mathcal{H}_\infty}$ is equal to the $\mathcal{L}_2$ induced (system) norm related to the input $u_1(t)$ and the output $y_i(t)$, as follows:

$$\|P_i(s)\|_{\mathcal{H}_\infty} = \sup_{u_1 \neq 0} \frac{\|y_i(t)\|_{\mathcal{L}_2}}{\|u_1(t)\|_{\mathcal{L}_2}} \tag{15}$$

where the $\mathcal{L}_2$ norm is defined on the interval $t \in [0, \infty)$. Hence

$$\begin{aligned} \|y_i(t)\|_{\mathcal{L}_2} &\leq \|P_i(s)\|_{\mathcal{H}_\infty} \|u_1(t)\|_{\mathcal{L}_2} \\ &\leq \max_{i \in S_m} \|P_i(s)\|_{\mathcal{H}_\infty} \|u_1(t)\|_{\mathcal{L}_2}. \end{aligned} \tag{16}$$

Note that (16) is not conservative, in the sense that there is always a subsystem $i \in S_m$ and a specific signal $u_1(t)$ for which the equality holds, due to (15). Therefore, according to Definition 1 and under the conditions mentioned in Assumption 1, the existence of $\max_{i \in S_m} \|P_i(s)\|_{\mathcal{H}_\infty}$, for all $m \in \mathbb{N}$, is a necessary and sufficient condition for $\mathcal{L}_2$ string stability of the interconnected system (9).

If an infinite-length string consisting of linear *unidirectionally coupled* systems has a bounded output response to a bounded input, then also finite-length strings have a bounded output response. It therefore suffices to consider only the infinite-length string instead of all possible string lengths $m \in \mathbb{N}$. The sets S_m, $m \in \mathbb{N}$, over which the inequality (10) must hold, can be then simplified to a single set $\mathbb{N}$. As a result, the following string stability condition can be formulated.

Condition 1 ($\mathcal{L}_2$ String Stability): The interconnected system (9), with input–output representation (13), is $\mathcal{L}_2$ string stable, under the condition mentioned in Assumption 1, if and only if

$$\sup_{i \in \mathbb{N}} \|P_i(s)\|_{\mathcal{H}_\infty} < \infty. \tag{17}$$

Assuming functional controllability [17] of the system (13) for $i = 1$, i.e., $P_1^{-1}(s)$ exists (which is why the system is assumed to be square), the transfer function $\Theta_i(s)$ from "input" $y_1(s)$ to output $y_i(s)$ can be defined according to

$$\Theta_i(s) := P_i(s)P_1^{-1}(s) \tag{18}$$

such that $P_i(s) = \Theta_i(s)P_1(s)$. The following condition for semi-strict $\mathcal{L}_2$ string stability can now be formulated.

Condition 2 (Semi-Strict $\mathcal{L}_2$ String Stability): Subject to Assumption 1, the interconnected system (13) is semi-strictly $\mathcal{L}_2$ string stable with respect to its input u_1 if and only if

$$\|P_1(s)\|_{\mathcal{H}_\infty} < \infty \tag{19a}$$

$$\|\Theta_i(s)\|_{\mathcal{H}_\infty} \leq 1 \quad \forall\, i \in \mathbb{N}\backslash\{1\}. \tag{19b}$$

The sufficiency of the conditions (19a) and (19b) for $\mathcal{L}_2$ string stability follows from the fact that $\|P_i(s)\|_{\mathcal{H}_\infty} \leq \|\Theta_i(s)\|_{\mathcal{H}_\infty} \|P_1(s)\|_{\mathcal{H}_\infty}$ and Condition 1. Furthermore, since $y_i(s) = \Theta_i(s)y_1(s)$, it follows that the system is also semi-strictly $\mathcal{L}_2$ string stable if (19b) holds. The necessity of condition (19a) is immediate. Moreover, if (19b) is not satisfied for some i, it follows that $\|y_i(t)\|_{\mathcal{L}_2} > \|y_1(t)\|_{\mathcal{L}_2}$ for some $y_1(t)$, indicating the necessity of condition (19b).

Along the same line of thought, the transfer function $\Gamma_i(s)$ from $y_{i-1}(s)$ to $y_i(s)$ is introduced, assuming functional controllability of $P_{i-1}(s)$, according to

$$\Gamma_i(s) := P_i(s)P_{i-1}^{-1}(s) \tag{20}$$

which is referred to as the string stability complementary sensitivity. This leads to the following strict $\mathcal{L}_2$ string stability condition, a formal proof of which is given in [13].

Condition 3 (Strict $\mathcal{L}_2$ String Stability): Subject to Assumption 1, the system (13) is strictly $\mathcal{L}_2$ string stable with respect to its input u_1 if and only if

$$\|P_1(s)\|_{\mathcal{H}_\infty} < \infty \tag{21a}$$

$$\|\Gamma_i(s)\|_{\mathcal{H}_\infty} \leq 1 \quad \forall\, i \in \mathbb{N}\backslash\{1\}. \tag{21b}$$

Conditions 2 and 3 now provide a basis for controller design by means of $\mathcal{H}_\infty$ optimization for the vehicle-following control problem, as introduced in the next section.

IV. $\mathcal{H}_\infty$ Control Problem

Before casting the platoon control problem into the $\mathcal{H}_\infty$ synthesis framework [15], the general $\mathcal{H}_\infty$ control configuration, as shown in Fig. 3, is described first. Here, the plant $\mathcal{P}$ is

[2] According to the maximum modulus theorem [15], the $\mathcal{H}_\infty$ norm can be computed by evaluation of $\bar{\sigma}(P_i(s))$ along the imaginary axis, i.e., $\sup_{Re(s)>0} \bar{\sigma}(P_i(s)) = \sup_{\omega \in \mathbb{R}} \bar{\sigma}(P_i(j\omega))$. Therefore, s and $j\omega$ are sometimes used interchangeably in this paper.

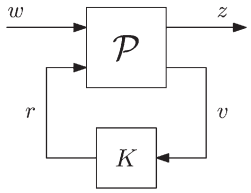

Fig. 3. $\mathcal{H}_\infty$ optimal control configuration.

the system to be controlled, whereas w denotes the exogenous inputs, r denotes the control signals, z denotes the exogenous outputs, and v denotes the controller inputs, i.e.,

$$\begin{pmatrix} z(s) \\ v(s) \end{pmatrix} = \mathcal{P}(s) \begin{pmatrix} w(s) \\ r(s) \end{pmatrix}. \tag{22}$$

In the scope of the platooning problem, the control signal is scalar and equal to $r = \xi_i$, and the controller inputs are equal to $v^T = (e_i \; u^*_{i-1} \; \dots \; u^*_{i-k})$, corresponding to (7).

The feedback loop is closed by a controller K according to

$$r(s) = K(s)v(s) \tag{23}$$

upon which the controlled system is described by

$$z(s) = N(s)w(s) \tag{24}$$

with $N = \mathcal{P}_{11} + \mathcal{P}_{12}K(I - \mathcal{P}_{22}K)^{-1}\mathcal{P}_{21}$, omitting the argument s for readability. Here, $\mathcal{P}(s)$ is partitioned in block matrices $\mathcal{P}_{ij}(s)$, $i, j \in \{1, 2\}$, of dimensions corresponding to the inputs and outputs in (22). $N(s)$ is known as the (lower) linear fractional transformation (LFT) [15]. $\mathcal{H}_\infty$ optimal control now involves finding a controller $K_{\text{opt}}(s)$, such that

$$K_{\text{opt}}(s) = \arg\min_K \|N(K)\|_{\mathcal{H}_\infty} \tag{25}$$

yielding a stable system without cancellation of unstable or marginally stable plant poles by the controller (i.e., *internally* stable). To this end, either a Riccati-based approach or a linear-matrix-inequality-based approach can be applied [18]. The specific form of the $\mathcal{H}_\infty$ synthesis objective in (25) motivates the choice for this type of controller design strategy for the platoon problem, since the conditions (19b) and (21b) for (semi-)strict $\mathcal{L}_2$ string stability are also concerned with minimizing the $\mathcal{H}_\infty$ norm of a transfer function. Hence, if the exogenous input w and the exogenous output z are chosen such that $N(s)$ contains either $\Theta_i(s)$ or $\Gamma_i(s)$, then (semi-)strict $\mathcal{L}_2$ string stability is actively pursued by the controller synthesis procedure, and condition (19b) or (21b) is satisfied if $N(s)$ in (24) satisfies $\|N(s)\|_{\mathcal{H}_\infty} \leq 1$. In addition, the error e_i must be included in z, in view of the vehicle-following objective (3). The specific choices for w and z, however, depend on the particular communication topology under study, as will be further described in the next section.

V. Controller Synthesis for String-Stable Platooning

Having formulated the control problem, a platooning controller for a one- and a two-vehicle look-ahead topology is designed. The motivation for the latter is to investigate the benefits of a more complex communication topology, while also illustrating that the controller synthesis procedure is able to go beyond the basic one-vehicle look-ahead topology.

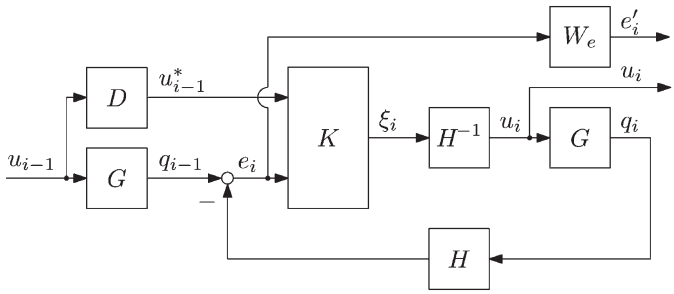

Fig. 4. One-vehicle look-ahead CACC configuration.

A. One-Vehicle Look-Ahead Topology

In case of the one-vehicle look-ahead CACC scheme, the input u_{i-1} of the preceding vehicle is employed to obtain string stability. Since u_{i-1} and q_{i-1} are related through the vehicle model $G(s)$ (bearing in mind the homogeneity of the vehicle dynamics), the block scheme arises, as shown in Fig. 4.

The (weighted) distance error e_i is chosen as the first output, since it directly relates to the vehicle-following objective. The weighting is implemented in the Laplace domain by a function $W_e(s)$, providing a means to further specify the control objectives as commonly employed in $\mathcal{H}_\infty$ controller synthesis. Consequently, $e_i'(s) = W_e(s)e_i(s)$ becomes the first exogenous output. Next, since u_{i-1} is the exogenous input, the string stability complementary sensitivity is chosen as

$$\Gamma_i(s) = \frac{u_i(s)}{u_{i-1}(s)} \tag{26}$$

which is why u_i is taken as the second exogenous output, having the advantage that the control effort is minimized at the same time. The controller design thus aims for strict $\mathcal{L}_2$ string stability. Hence, Condition 3 applies. Note that $P_1(s) = 1$, due to the choice of u_i as the relevant output for string stability; therefore, condition (21a) is satisfied by definition.

The (mixed-sensitivity) $\mathcal{H}_\infty$ control problem is now to compute a stabilizing controller $K(s) = (K_{\text{fb}}(s) \; K_{\text{ff}}(s))$, with

$$\xi_i(s) = (K_{\text{fb}}(s) \; K_{\text{ff}}(s)) \begin{pmatrix} e_i(s) \\ u^*_{i-1}(s) \end{pmatrix} \tag{27}$$

such that $\|N(s)\|_{\mathcal{H}_\infty}$ is minimized, where

$$\begin{pmatrix} e_i'(s) \\ u_i(s) \end{pmatrix} = \begin{pmatrix} W_e(s)S(s) \\ \Gamma(s) \end{pmatrix} u_{i-1}(s) := N(s)u_{i-1}(s). \tag{28}$$

Here, the sensitivity is

$$S(s) = \tilde{S}(s)G(s)\,(1 - K_{\text{ff}}(s)D(s)) \tag{29}$$

and the string stability complementary sensitivity is

$$\Gamma(s) = \tilde{S}(s)H^{-1}(s)\,(K_{\text{fb}}(s)G(s) + K_{\text{ff}}(s)D(s)) \tag{30}$$

with

$$\tilde{S}(s) = (1 + K_{\rm fb}(s)G(s))^{-1}. \tag{31}$$

It is noted that $\Gamma(s)$ does not depend on the index i, which can be readily understood when realizing that the block scheme in Fig. 4 holds for all vehicles $i > 1$. As desired, the synthesized controller is also independent of i.

From $N(s)$ in (28), it follows that

$$\|N(s)\|_{\mathcal{H}_\infty} = \gamma \Rightarrow \|\Gamma(s)\|_{\mathcal{H}_\infty} \leq \gamma. \tag{32}$$

According to condition (21b), string stability is thus obtained for any value $\gamma \leq 1$. On the other hand, if the vehicle-following objective is realized, it must hold that $\lim_{\omega\to 0}(v_i(j\omega) - v_{i-1}(j\omega)) = 0$, where $\omega \in \mathbb{R}$ is the frequency. Also taking into account the homogeneity of the vehicle dynamics, due to which $u_i(j\omega)/u_{i-1}(j\omega) = v_i(j\omega)/v_{i-1}(j\omega)$, this implies

$$\lim_{\omega\to 0} |\Gamma(j\omega)| = 1 \Rightarrow \|\Gamma(s)\|_{\mathcal{H}_\infty} \geq 1. \tag{33}$$

From (32) and (33), it thus follows that

$$\|N(s)\|_{\mathcal{H}_\infty} = 1 \tag{34}$$

is the $\mathcal{H}_\infty$ synthesis objective for the design of a strictly $\mathcal{L}_2$ string-stabilizing controller. Note that, considering (33) and $N(s)$ in (28), (34) is a sufficient condition for strict $\mathcal{L}_2$ string stability and asymptotic tracking.

The weighting function $W_e(s)$ in (28) balances vehicle-following performance against string stability. However, since the focus here is on string stability, $W_e(s) = 1$ is chosen, thus equally penalizing the amplification of disturbances in u_{i-1} over the entire frequency range. Furthermore, the vehicle parameters are set to $\tau = 0.1$ s and $\phi = 0.2$ s, with communication delay $\theta = 0.02$ s (see Section VI). In addition, both the vehicle and the communication delay are described by a third-order Padé approximation, yielding a sufficiently accurate phase in the frequency interval of interest. Finally, a design time headway $h = 1$ s is chosen, being the standardized minimum for ACC [19]. The $\mathcal{H}_\infty$ optimization procedure then yields a tenth-order state-space model of the controller. This controller is reduced by removing the states that are associated with small Hankel singular values, upon which the controller is written as a transfer function $K(s)$. After manually removing the poles and zeros that are outside the frequency region of interest and that do not significantly influence the string stability properties of the controlled system, the final controller design reads

$$K_{\rm fb}(s) = \frac{2.6880(s+23.22)(s+10)(s+1)(s+0.3646)}{(s+24.65)(s+5.926)(s+5.049)(s+0.9947)}$$
$$K_{\rm ff}(s) = \frac{1.0391(s+24.1)(s+7.233)(s+4.051)(s+1)}{(s+24.65)(s+5.926)(s+5.049)(s+0.9947)}. \tag{35}$$

This controller realizes a stable platooning system, which can, e.g., readily be checked by computing the poles of $\Gamma(s)$. Because the controller does not cancel the marginally stable poles of $G(s)$, the system is also internally stable.

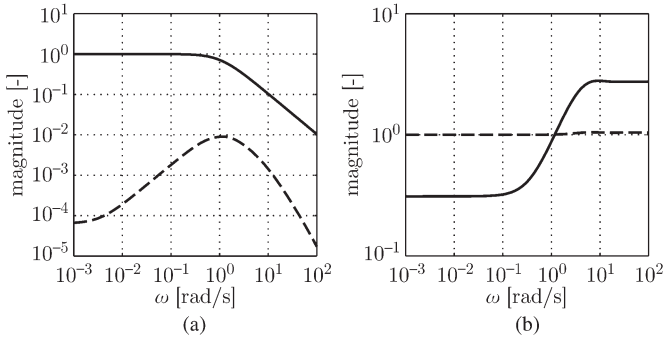

Fig. 5. Frequency response magnitude. (a) $N(j\omega)$: $|\Gamma(j\omega)|$ (solid) and $|S(j\omega)|$ (dashed). (b) $K(j\omega)$: $|K_{\rm fb}(j\omega)|$ (solid) and $|K_{\rm ff}(j\omega)|$ (dashed).

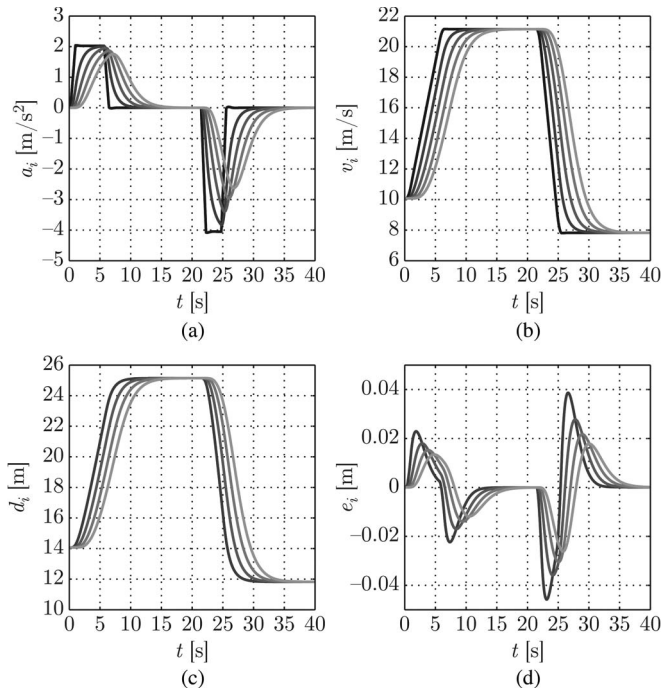

Fig. 6. Time responses of (a) acceleration $a_i(t)$ and (b) velocity $v_i(t)$ (black–light gray: $i = 1, 2, \ldots, 5$) and of (c) distance $d_i(t)$ and (d) distance error $e_i(t)$ (dark–light gray: $i = 2, 3, 4, 5$).

Indeed, with this controller, $\|N(s)\|_{\mathcal{H}_\infty} = 1$ is obtained. This is confirmed in Fig. 5(a), showing that $|S(j\omega)| \leq 1$ and $|\Gamma(j\omega)| \leq 1$, hence realizing strict $\mathcal{L}_2$ string stability. In addition, Fig. 5(b) shows the controller magnitudes $|K_{\rm fb}(j\omega)|$ and $|K_{\rm ff}(j\omega)|$, which illustrates that the feedforward gain is very close to 1 over the entire frequency range. This, in fact, corresponds to the controller designed in [12], where the feedforward gain was chosen identical to 1. Note that the magnitude response $|K_{\rm fb}(j\omega)|$ exhibits a slope of approximately $+1$ around $\omega = 1$ rad/s, indicating that the feedback controller contains a differential action.

Fig. 6 shows the time responses of five vehicles for $h = 1$ s, with vehicle 1, which is velocity controlled (refer to Section VI), performing a smooth velocity step upward and downward, based on a trapezoidal acceleration profile. The acceleration responses (which are very similar to the control actions, given the relatively small values for τ and ϕ) clearly

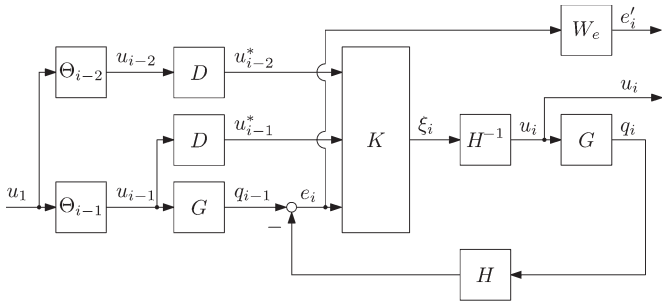

Fig. 7. Two-vehicle look-ahead CACC configuration.

show a decreasing amplitude along the string, indicating *strict* $\mathcal{L}_2$ string-stable behavior. This is confirmed by the absence of overshoot in the velocity responses. Furthermore, the distance responses reflect the velocity-dependent spacing policy, whereas from the distance error response, it can be concluded that the vehicle-following objective is reached.

It is noted that, although (semi-)strict $\mathcal{L}_2$ string stability characterizes the propagation of the effects of input disturbances, satisfying this property also implies that the system outputs are bounded with respect to bounded initial condition perturbations. In other words, no (string-unstable) amplification of initial condition perturbations can occur. Moreover, since the controlled system is linear and time invariant, the initial condition response is characterized by the transfer function that also describes the input–output behavior, i.e., $\Gamma(s)$. For these reasons, initial condition perturbations are not explicitly considered here.

B. Two-Vehicle Look-Ahead Topology

To illustrate the design procedure in case of a more complex information topology and to investigate the possible benefits of this topology with respect to string stability, this section is concerned with a two-vehicle look-ahead topology, taking an additional controller input u_{i-2}^* into account. In this case, however, u_{i-1}^* and u_{i-2}^* are not independent inputs, since they both depend on u_{i-3}^*, whereas u_{i-2}^* and u_{i-3}^* both depend on u_{i-4}^*, etc. In other words, a single-vehicle subsystem with an independent input cannot be isolated, as was the case with the one-vehicle look-ahead topology. Consequently, the lead vehicle input u_1 is chosen to be the independent input, yielding the block scheme as shown in Fig. 7. In this figure, it is shown that the transfer function $\Theta_i(s)$, defined in (18), is equal to

$$\Theta_i(s) = \frac{u_i(s)}{u_1(s)}. \tag{36}$$

Again choosing the exogenous outputs to be the weighted distance error e_i' and the desired acceleration u_i, whereas u_1 becomes the exogenous input, the mixed-sensitivity $\mathcal{H}_\infty$ control problem now involves computing a stabilizing controller $K(s) = (K_{\text{fb}}(s)\ K_{\text{ff},1}(s)\ K_{\text{ff},2}(s))$ according to

$$\xi_i(s) = \begin{pmatrix} K_{\text{fb}}(s) & K_{\text{ff},1}(s) & K_{\text{ff},2}(s) \end{pmatrix} \begin{pmatrix} e_i(s) \\ u_{i-1}^*(s) \\ u_{i-2}^*(s) \end{pmatrix} \tag{37}$$

such that $\|N_i(s)\|_{\mathcal{H}_\infty}$ is minimized, with

$$\begin{pmatrix} e_i'(s) \\ u_i(s) \end{pmatrix} = \begin{pmatrix} W_e(s)S_i(s) \\ \Theta_i(s) \end{pmatrix} u_1(s) := N_i(s)u_1(s). \tag{38}$$

Here, the sensitivity $S_i(s)$ is equal to (omitting the argument s)

$$S_i = \tilde{S}G\left((1 - K_{\text{ff},1}D)\,\Theta_{i-1} - K_{\text{ff},2}D\Theta_{i-2}\right) \tag{39}$$

with $\tilde{S}$ as in (31), whereas $\Theta_i(s)$, $i \geq 3$, is equal to

$$\Theta_i = \tilde{S}H^{-1}\left((K_{\text{fb}}G + K_{\text{ff},1}D)\,\Theta_{i-1} + K_{\text{ff},2}D\Theta_{i-2}\right) \tag{40}$$

with $\Theta_1(s) = 1$ and $\Theta_2(s) = \Gamma_2(s)$ by definition. Assuming that the second vehicle, having only one preceding vehicle, is controlled using the one-vehicle look-ahead controller (35), it follows that $\Gamma_2(s) = \Gamma(s)$ according to (30).

The controller design thus naturally aims for semi-strict $\mathcal{L}_2$ string stability, which is subject to Condition 2, where the inequality (19a) is met by definition since $P_1(s) = 1$. As opposed to the one-vehicle look-ahead case, $N_i(s)$ now appears to depend on the vehicle index i, and so will the synthesized controller. Consequently, the $\mathcal{H}_\infty$ optimal controller depends on the position in the platoon of the specific vehicle, which is undesired in view of the ad hoc platooning approach. This property is a direct consequence of the fact that a single-vehicle subsystem with an independent input cannot be isolated, as mentioned before. To overcome this limitation, a controller is synthesized for the third vehicle only, being the first vehicle in the string with two preceding vehicles, aiming for $\|N_3(s)\|_{\mathcal{H}_\infty} = 1$. This controller is then applied to all upstream vehicles $i \geq 4$ as well, after which the resulting string stability properties will be analyzed through the assessment of condition (19b).

Using the same motivation as before, $W_e(s) = 1$ is chosen. The controller is synthesized with the model parameters from the previous subsection and a design time headway of $h = 1$ s, while employing a third-order Padé approximation for the vehicle and the communication delay. In addition, $\Gamma(s)$ is approximated by $H^{-1}(s)$ (by substituting $K_{\text{ff}}(s) = 1$ with communication delay $\theta = 0$) to decrease the order of the controller. As a result, the following reduced-order controller is obtained:

$$\begin{aligned}
K_{\text{fb}} &= \frac{1.8517(s+23.22)(s+10)(s+1.39)(s+1)(s+0.3893)}{(s+23.97)(s+8.201)(s+2.783)(s+1.272)(s+1.185)} \\
K_{\text{ff},1} &= \frac{0.4299(s+23.22)(s+10.03)(s+1)(s^2+2.904s+3.617)}{(s+23.97)(s+8.201)(s+2.783)(s+1.272)(s+1.185)} \\
K_{\text{ff},2} &= \frac{0.2664(s+23.14)(s+10.49)(s+1)(s^2+2.411s+7.145)}{(s+23.97)(s+8.201)(s+2.783)(s+1.272)(s+1.185)}.
\end{aligned} \tag{41}$$

This controller realizes an internally stable system since the poles of $\Theta_3(s)$ are in the left half-plane, whereas the controller does not cancel the marginally stable poles of $G(s)$. Furthermore, $\|N_3(s)\|_{\mathcal{H}_\infty} = 1$ is obtained, which is confirmed in Fig. 8(a), showing that $|S_3(j\omega)| \leq 1$ and $|\Theta_3(j\omega)| \leq 1$. In

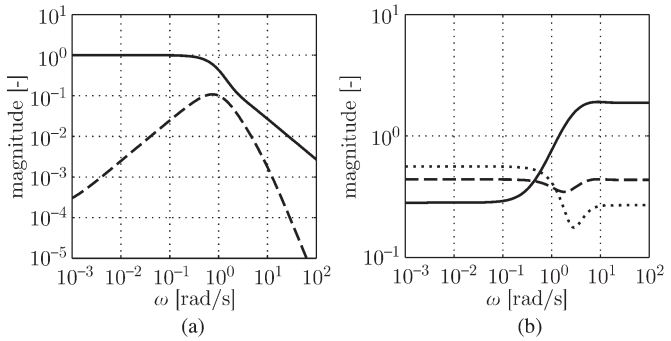

Fig. 8. Frequency response magnitude. (a) LFT $N(j\omega) : |\Theta_3(j\omega)|$ (solid) and $|S_3(j\omega)|$ (dashed). (b) Controller $K(j\omega) : |K_{\rm fb}(j\omega)|$ (solid), $|K_{{\rm ff},1}(j\omega)|$ (dashed), and $|K_{{\rm ff},2}(j\omega)|$ (dotted).

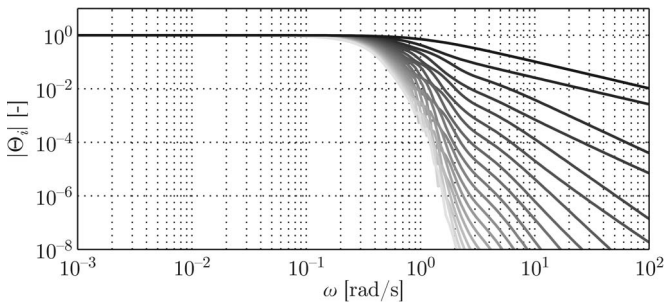

Fig. 9. Frequency response magnitude of $\Theta_i(j\omega)$ (black–light gray: $i = 2, 3, \ldots, 20$).

addition, Fig. 8(b) shows the controller magnitudes $|K_{\rm fb}(j\omega)|$, $|K_{{\rm ff},1}(j\omega)|$, and $|K_{{\rm ff},2}(j\omega)|$, from which it can be concluded that a weighted feedforward of u_1 and u_2 is obtained. Note that $|K_{{\rm ff},1}(j\omega) + K_{{\rm ff},2}(j\omega)| \to 1$ for $\omega \to 0$.

For semi-strict $\mathcal{L}_2$ string stability, condition (19b) must hold, which requires to investigate $\|\Theta_i(s)\|_{\mathcal{H}_\infty}$ for $i \geq 4$. This can be done by numerical evaluation of $|\Theta_i(j\omega)|$ using (40) with initial conditions $\Theta_1(j\omega) = 1$ and $\Theta_2(j\omega) = \Gamma(j\omega)$, the result of which is shown in Fig. 9 for $i = 1, 2, \ldots, 20$. This figure shows a trend of decreasing magnitude $|\Theta_i(j\omega)|$ for increasing i (also for $i > 20$), confirming semi-strict $\mathcal{L}_2$ string stability.

Fig. 10 shows the time responses of five vehicles to a smooth velocity step of vehicle 1, which is the same as the one used in Fig. 6, obtained with $h = 1$ s. It appears that the responses of the acceleration, the velocity, and the distance are very similar to those of the one-vehicle look-ahead controlled system, as shown in Fig. 6. The distance error response, however, shows significantly larger error amplitudes, although asymptotic tracking behavior is certainly obtained. Note that, using (26) and (36), the string stability complementary sensitivity is equal to

$$\Gamma_i(s) = \Theta_i(s)\Theta_{i-1}^{-1}(s) \tag{42}$$

based on which it can be established that the controlled system is not strictly $\mathcal{L}_2$ string stable (not shown here). Nevertheless, $|\Gamma_i(j\omega)|$ slightly exceeds 1 only for $i \geq 10$ and only at frequencies beyond the bandwidth of $\Theta_i(j\omega)$, which is why this effect only becomes visible in the distance error responses.

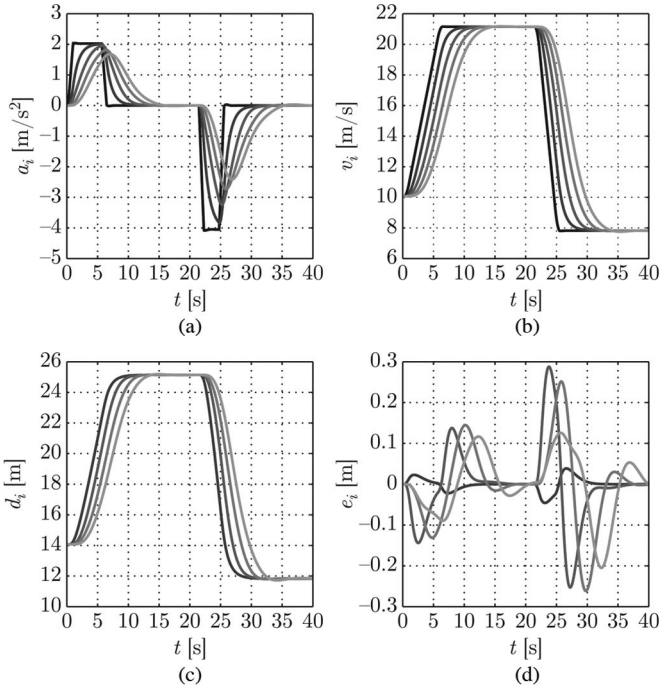

Fig. 10. Time responses of (a) acceleration $a_i(t)$ and (b) velocity $v_i(t)$ (black–light gray: $i = 1, 2, \ldots, 5$) and of (c) distance $d_i(t)$ and (d) distance error $e_i(t)$ (dark–light gray: $i = 2, 3, 4, 5$).

C. Performance Comparison

Based on the results so far, the two-vehicle look-ahead strategy does not seem to improve upon the string stability properties of the one-vehicle look-ahead strategy for this particular case study. To further compare both communication topologies, the influence of the time headway h on string stability in relation to the communication delay θ is investigated.

For the one-vehicle look-ahead controller, it appears that the factor $H^{-1}(s) = 1/(hs + 1)$ in $\Gamma(s)$ [see (30)] decreases the peak value of the magnitude of the remaining transfer functions in $\Gamma(s)$, the effect of which is smaller for decreasing values of h. Hence, with a communication delay $\theta > 0$, a minimum time headway $h_{\min}$ must exist that realizes string stability.[3] Indeed, it appears that, with $\theta = 0.02$ s, the controlled system is string stable for $h \geq h_{\min} = 0.15$ s. However, for the two-vehicle look-ahead topology, a significantly larger value of $h_{\min} = 0.39$ s is found. This result can be understood as follows: Without communication delay $(D(s) = 1)$, while approximating the feedforward transfer function by $K_{\rm ff}(s) = 1$, the one-vehicle look-ahead sensitivity (29) is equal to $S = 0$, indicating perfect following behavior. Consequently, additional information, which is obtained from the second preceding vehicle, would not yield additional benefit. On the other hand, for increasing communication delay, one may expect to benefit from the information of the second preceding vehicle, because it provides "preview" disturbance information, due to the fact

[3]Without communication delay, i.e., $D(s) = 1$, while substituting $K_{\rm ff}(s) = 1$, $\Gamma(s) = H^{-1}(s)$ is obtained, such that $\|\Gamma(s)\|_{\mathcal{H}_\infty} = 1$, regardless of the value of the time headway h.

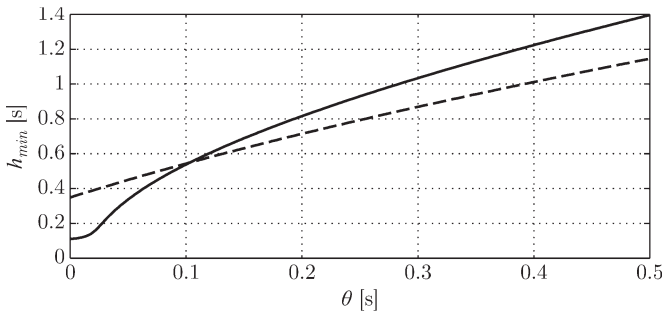

Fig. 11. Minimum headway $h_{\min}$ as a function of communication delay θ for one-vehicle and two-vehicle look-ahead control (solid and dashed, respectively).

Fig. 12. Experimental vehicle platoon, consisting of three CACC-equipped passenger vehicles.

that the delay is identical for all vehicles. This intuition is confirmed by determining the minimum string-stable time headway $h_{\min}$ as a function of the communication delay θ, the result of which is shown in Fig. 11. This figure has been obtained by taking a fixed value for θ and then searching for the smallest value of h, such that $\|\Gamma(s)\|_{\mathcal{H}_\infty} = 1$ for the one-vehicle look-ahead case, or $\|\Theta_3(s)\|_{\mathcal{H}_\infty} = 1$ for the two-vehicle look-ahead case. Indeed, it appears that above a certain break-even communication delay, here about 0.1 s, the two-vehicle look-ahead topology allows for smaller time headways in view of string stability. It can therefore be concluded that a multiple-vehicle look-ahead scheme provides a benefit with respect to minimum string-stable time headway when the communication delay exceeds a certain threshold. Hence, it may be worthwhile, in practice, to actively switch between communication topologies and corresponding controllers, depending on the actual latency of the wireless communication.

VI. Experimental Validation

Both controllers have been implemented in a platoon of three passenger vehicles, as shown in Fig. 12, equipped with a prototype CACC system. This system encompasses a forward-looking radar, wireless communications according to the ETSI ITS G5 standard [20], and a computer system that executes the CACC controller and allows for computer-controlled vehicle acceleration through interaction with the native vehicle control system [12]. This section presents experimentally obtained frequency and time responses to validate the theoretical results regarding string stability.

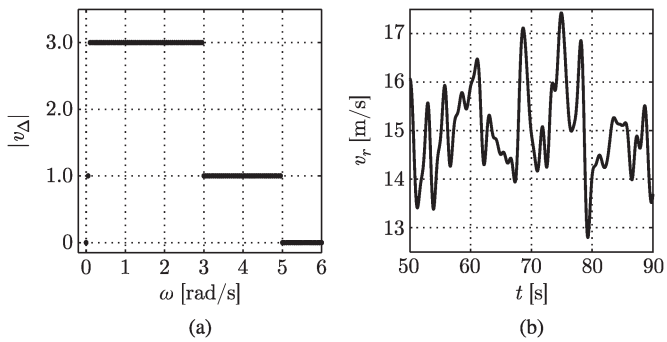

Fig. 13. Test signal: (a) magnitude $|v_\Delta(j\omega)|$ and (b) excerpt of the corresponding time-domain signal $v_r(t)$.

A. Frequency Response Experiments

The lead vehicle is required to follow a predefined velocity profile $v_r(t)$, which is designed to excite the follower vehicles in the frequency region of interest for the assessment of string stability. To this end, the frequency-domain amplitude $|v_\Delta(j\omega)|$ of a zero-mean velocity profile $v_\Delta(t)$ is chosen, as displayed in Fig. 13(a), covering the frequency interval [0.05, 5] rad/s, while emphasizing the region [0.1, 3] rad/s because it is expected that string stability may be violated in this interval. Upon choosing a uniformly distributed random phase for each value of $|v_\Delta(j\omega)|$, the frequency-domain signal is transformed to the time domain, which, after scaling and adding a nominal velocity of 15 m/s, yields the velocity profile $v_r(t)$, as partly depicted in Fig. 13(b). Here, the amplitude of the velocity variations is scaled, such that the acceleration covers the interval $[-3, 3]$ m/s^2. v_r is subsequently applied as the desired velocity for a velocity-feedback controller implemented in the lead vehicle, where the performance is greatly enhanced by adding a feedforward signal $u_{\rm ff}$ on the vehicle's input, which is derived from (4), according to

$$u_{\rm ff}(t) = \tau \ddot{v}_r(t+\theta) + \dot{v}_r(t+\theta) \tag{43}$$

thus taking care that the frequency content of the velocity profile remains intact. Note that the same velocity controller was used in the time-domain simulations presented in Section V.

Based on earlier experiments, the round-trip time of a wireless message appeared to be 40 ms on average, which is primarily determined by the update rate of 25 Hz of the wireless communication network. Consequently, $\theta \approx 0.02$ s, as used earlier in the controller design.

The first experiment is conducted with two vehicles, focusing on the one-vehicle look-ahead topology in which the follower vehicle is equipped with the controller (35). Upon measuring the communicated input $u_1^*(t)$ of the lead vehicle and the local input $u_2(t)$ of the follower vehicle, the magnitude $|\Gamma(j\omega)|$ of the string stability complementary sensitivity is estimated, employing Welch's averaged periodogram method. Note that the delayed input $u_1^*(t)$ can be used instead of the actual input $u_1(t)$ since only the magnitude of $\Gamma(j\omega)$ is of interest. Fig. 14(a) shows the theoretical magnitude according to (30) and the estimated magnitude, with time headway $h = 1$ s. This figure clearly shows the similarity between both frequency response magnitudes, thus validating the theoretical results. Note that the

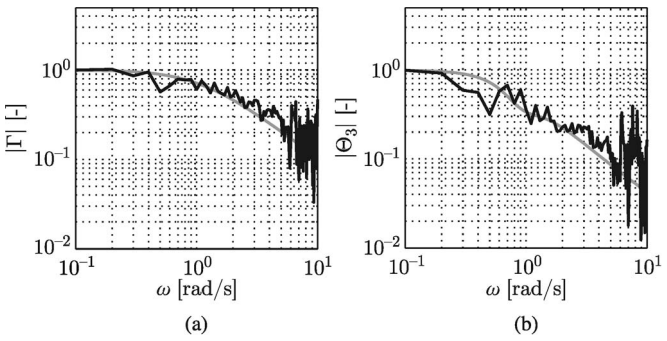

Fig. 14. Estimated (black) and theoretical (gray) frequency response magnitude. (a) $|\Gamma(j\omega)|$ for the one-vehicle look-ahead topology. (b) $|\Theta_3(j\omega)|$ for the two-vehicle look-ahead topology. $h = 1.0$ s in both cases.

quality of the estimate strongly degrades for $\omega > 5$ rad/s, which is of course due to the fact that the test signal does not contain any frequency content in this region.

The same experiment is carried out with three vehicles. Here, the second vehicle is controlled by the one-vehicle look-ahead controller (35), whereas the third vehicle is controlled by the two-vehicle look-ahead controller (41). The theoretical magnitude $|\Theta_3(j\omega)|$ according to (40) and the resulting estimated frequency response magnitude are shown in Fig. 14(b), with $h = 1$ s. Again, the experimental results are consistent with the theoretical results.

B. Time Response Experiments

The second type of experiment aims to validate the simulated time responses, as shown in Section V. First, the simulation shown in Fig. 6 for the one-vehicle look-ahead controlled system with $h = 1$ s is repeated, in practice, with three vehicles, where the first vehicle is velocity controlled with the same controller used in the simulation, which is subject to the same desired velocity profile. Fig. 15 shows the measured acceleration, velocity, distance and distance error, which can be directly compared with the simulation results in Fig. 6.

The acceleration, velocity, and distance are clearly very similar to those shown in the simulation, thus confirming $\mathcal{L}_2$ string stability. Furthermore, there is no overshoot during the acceleration section of the test scenario and (almost) no undershoot at the rather strong deceleration, thus ensuring safe behavior within the operational range of the CACC system.

The distance error, however, appears to be significantly larger than in the simulation. This is partly caused by measurement noise, the level of which is indicated by the constant-velocity sections of the test scenario. Another cause is the following. It is known that, due to the feedforward of the preceding vehicle's input, the system behavior is sensitive to variations in the vehicle dynamics (4) along the string. Although all test vehicles are of the same type, these "inhomogeneities" occur, among others, because the batteries of the hybrid drivelines do not have the same state of charge. Since particularly the second vehicle in the string shows a relatively large distance error, it is therefore concluded that the first vehicle behaves slightly differently than the other vehicles. This causes an error in the input feedforward for the second vehicle, but does not influence the third vehicle,

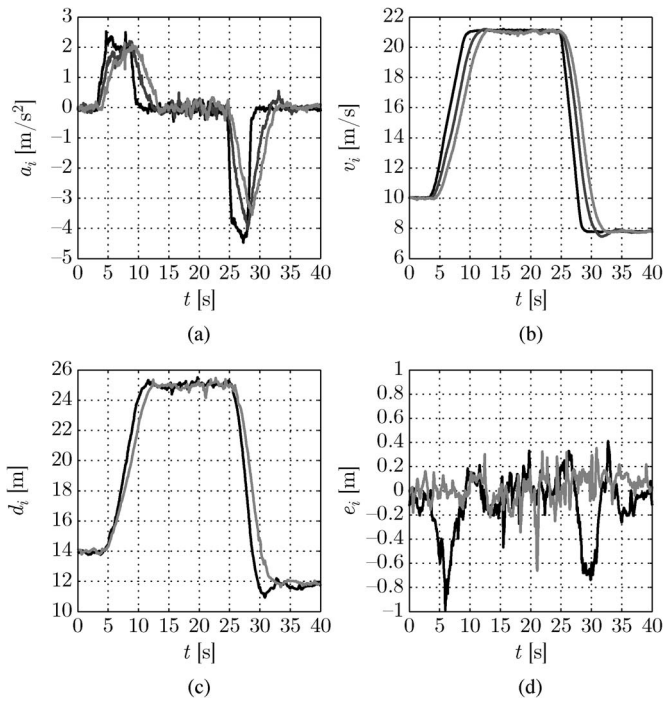

Fig. 15. One-vehicle look-ahead CACC time responses of (a) acceleration $a_i(t)$ and (b) velocity $v_i(t)$ (black–light gray: $i = 1, 2, 3$) and of (c) distance $d_i(t)$ and (d) distance error $e_i(t)$ (black, light gray: $i = 2, 3$).

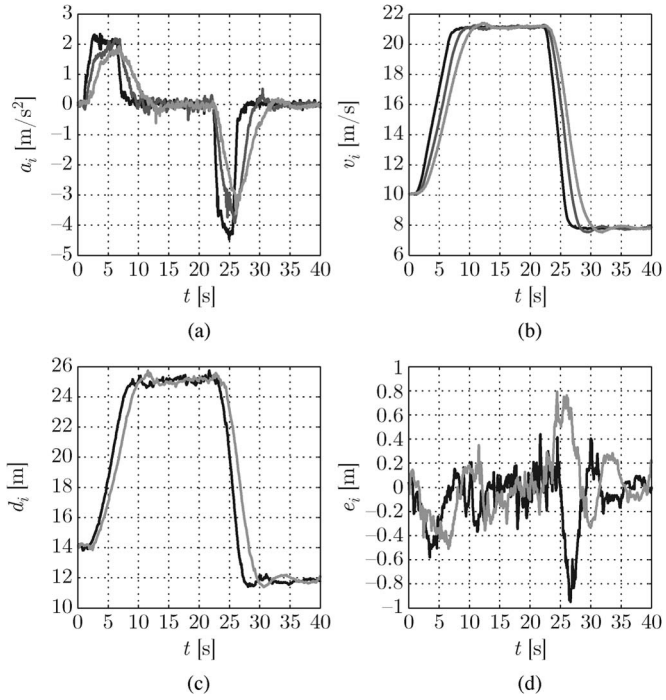

Fig. 16. Two-vehicle look-ahead CACC time responses of (a) acceleration $a_i(t)$ and (b) velocity $v_i(t)$ (black–light gray: $i = 1, 2, 3$) and of (c) distance $d_i(t)$ and (d) distance error $e_i(t)$ (black, light gray: $i = 2, 3$).

as shown by the responses in Fig. 15. Nevertheless, taking into account the high level of acceleration and deceleration, the designed controller performs at a satisfactory level.

Finally, the same experiment is performed with the two-vehicle look-ahead controller, the results of which are shown in Fig. 16, to be compared with Fig. 10. The aforementioned

remarks also apply here, apart form the fact that the inhomogeneity now influences both follower vehicles due to the communication topology. It is noted that the velocity and the distance are slightly less damped, as compared in the one-vehicle look-ahead case. This is also observed in Fig. 10.

VII. Conclusion

String stability is an important requirement for the design of controllers for vehicle platoons because it allows for short intervehicle following distances and scalability of the platoon with respect to its length. The application of the $\mathcal{H}_\infty$ synthesis framework appeared to allow for the explicit inclusion in the controller design specification of the $\mathcal{L}_2$ string stability requirement for linear cascaded systems, in general, and vehicle platoons in particular. As a result, strict (preceding to follower vehicle) $\mathcal{L}_2$ string-stable behavior was obtained for a one-vehicle look-ahead communication topology, whereas semi-strict (lead to follower vehicle) $\mathcal{L}_2$ string-stable behavior was realized for a two-vehicle look-ahead topology. In addition, it was found that the two-vehicle look-ahead topology provides a benefit with respect to minimum string-stable time headway when the communication delay exceeds a certain threshold.

Both controllers were evaluated, in practice, using a platoon of three passenger vehicles, which were specifically instrumented to test platooning controllers. A frequency- and time-domain analysis of the test results validated the theoretical results, while illustrating the practical feasibility of the presented approach at the same time.

Acknowledgment

The authors would like to thank Dr. T. Oomen for valuable discussions during the execution of the work presented in this paper and for his helpful comments.

References

[1] J. Piao and M. McDonald, "Advanced driver assistance systems from autonomous to cooperative approach," *Transp. Rev.*, vol. 28, no. 5, pp. 659–684, Sep. 2008.

[2] R. Rajamani and S. E. Shladover, "An experimental comparative study of autonomous and co-operative vehicle-follower control systems," *Transp. Res. Part C, Emerging Technol.*, vol. 9, no. 1, pp. 15–31, Feb. 2001.

[3] S. E. Shladover, D. Su, and X.-Y. Lu, "Impacts of cooperative adaptive cruise control on freeway traffic flow," in *Proc. 91st TRB Annu. Meet.*, Jan. 2012, pp. 1–17.

[4] R. Ramakers, K. Henning, S. Gies, D. Abel, and H. Max, "Electronically coupled truck platoons on German highways," in *Proc. IEEE Int. Conf. Syst., Man, Cybern.*, Oct. 2009, pp. 2409–2414.

[5] P. Seiler, A. Pant, and K. Hedrick, "Disturbance propagation in vehicle strings," *IEEE Trans. Autom. Control*, vol. 49, no. 10, pp. 1835–1842, Oct. 2004.

[6] R. Rajamani and C. Zhu, "Semi-autonomous adaptive cruise control systems," *IEEE Trans. Veh. Technol.*, vol. 51, no. 5, pp. 1186–1192, Sep. 2002.

[7] D. Swaroop, J. K. Hedrick, and S. B. Choi, "Direct adaptive longitudinal control of vehicle platoons," *IEEE Trans. Veh. Technol.*, vol. 50, no. 1, pp. 150–161, Jan. 2001.

[8] W. B. Dunbar and D. S. Caveney, "Distributed receding horizon control of vehicle platoons: Stability and string stability," *IEEE Trans. Autom. Control*, vol. 57, no. 3, pp. 620–633, Mar. 2012.

[9] P. Seiler and R. Sengupta, "An H_∞ approach to networked control," *IEEE Trans. Autom. Control*, vol. 50, no. 3, pp. 356–364, Mar. 2005.

[10] J. P. Maschuw, G. C. Kessler, and D. Abel, "LMI-based control of vehicle platoons for robust longitudinal guidance," in *Proc. 17th IFAC World Congr.*, Jul. 2008, pp. 12111–12116.

[11] G. J. L. Naus, R. P. A. Vugts, J. Ploeg, M. Molengraft, and M. Steinbuch, "String-stable CACC design and experimental validation: A frequency-domain approach," *IEEE Trans. Veh. Technol.*, vol. 59, no. 9, pp. 4268–4279, Nov. 2010.

[12] J. Ploeg, B. T. M. Scheepers, E. Nunen, N. Wouw, and H. Nijmeijer, "Design and experimental evaluation of cooperative adaptive cruise control," in *Proc. 14th Int. IEEE Conf. Intell. Transp. Syst.*, Oct. 2011, pp. 260–265.

[13] J. Ploeg, N. Wouw, and H. Nijmeijer, "$\mathcal{L}_p$ string stability of cascaded systems: Application to vehicle platooning," *IEEE Trans. Control Syst. Technol.*, vol. 22, no. 2, pp. 786–793, Mar. 2014.

[14] S. Öncü, N. Wouw, W. P. M. H. Heemels, and H. Nijmeijer, "String stability of interconnected vehicles under communication constraints," in *Proc. IEEE 51st Annu. Conf. Decision Control*, Dec. 2012, pp. 2459–2464.

[15] K. Zhou, J. C. Doyle, and K. Glover, *Robust and Optimal Control*. Englewood Cliffs, NJ, USA: Prentice Hall, 1996.

[16] H. K. Khalil, *Nonlinear Systems*, M. Horton, Ed. Upper Saddle River, NJ, USA: Prentice-Hall, 2000.

[17] R. V. Patel and N. Munro, *Multivariable System Theory and Design*. Oxford (UK), NY, USA: Pergamon Press, 1982.

[18] R. Y. Chiang and M. G. Safonov, *Robust Control Toolbox User's Guide*. Natick, MA, USA: The MathWorks, Inc., 1998.

[19] *International Organization for Standardization, Adaptive Cruise Control Systems—Performance Requirements and Test Procedures*, ISO Std. 15 622, Oct. 2002.

[20] E. G. Ström, "On medium access and physical layer standards for cooperative intelligent transport systems in Europe," *Proc. IEEE*, vol. 99, no. 7, pp. 1183–1188, Jul. 2011.

Jeroen Ploeg received the M.Sc. degree in mechanical engineering from Delft University of Technology, Delft, The Netherlands, in 1988. He is currently working toward the Ph.D. degree in real-time control of road vehicles for cooperative driving in the Department of Mechanical Engineering, Eindhoven University of Technology, Eindhoven, The Netherlands.

From 1989 to 1999, he was a Researcher with Koninklijke Hoogovens (currently Tata Steel), IJmuiden, The Netherlands, where his main interest was the dynamic process control of large-scale industrial plants. Since 1999, he has been a Senior Research Scientist with the Integrated Vehicle Safety Department, TNO, Helmond, The Netherlands. His current interests are focusing on control system design for advanced driver assistance systems and for path tracking of automatic guided vehicles.

Dipan P. Shukla received the B.Tech. degree in mechanical engineering from the Motilal Nehru National Institute of Technology, Allahabad, India, in 2008 and the M.Sc. degree in automotive engineering from the Eindhoven University of Technology, Eindhoven, The Netherlands, in 2012.

From 2008 to 2010, he was a Customer Support Engineer with Tata Motors Ltd., Kochi, India. In 2012, he performed his master's graduation project at the Integrated Vehicle Safety Department, TNO, Helmond, The Netherlands, where he focused on the control of vehicle platoons. Since 2013, he has been with the Continental Reifen Deutschland GmbH, Hannover, Germany, as an Engineer in the tires research and development graduate trainee program.

Nathan van de Wouw received the M.Sc. degree (with honors) and the Ph.D. degree in mechanical engineering from the Eindhoven University of Technology, Eindhoven, The Netherlands, in 1994 and 1999, respectively.

Since 1999, he has been with the Department of Mechanical Engineering, Eindhoven University of Technology, Eindhoven, The Netherlands, where he is an Assistant/Associate Professor with the Dynamics and Control Group. In 2000, he was with Philips Applied Technologies, Eindhoven, The Netherlands, and in 2001, he was with TNO, Delft, The Netherlands. He was a Visiting Professor with the University of California Santa Barbara, Santa Barbara, CA, USA, in 2006 and 2007; with the University of Melbourne, Parkville, Vic., Australia, in 2009 and 2010; and with the University of Minnesota, Minneapolis, MN, USA, in 2012 and 2013. He is the author of several books and a large number of journal and conference papers. His current research interests include the analysis and control of nonlinear/nonsmooth systems and networked control systems.

Dr. van de Wouw is currently an Associate Editor for Automatica.

Henk Nijmeijer (F'00) received the M.Sc. and Ph.D. degrees in mathematics from the University of Groningen, Groningen, The Netherlands, in 1979 and 1983, respectively.

From 1983 to 2000, he was with the Department of Applied Mathematics, University of Twente, Enschede, The Netherlands. Since 2000, he has been a Full Professor with the Eindhoven University of Technology, Eindhoven, The Netherlands, chairing the Dynamics and Control Group of the Department of Mechanical Engineering. He is the author of several books and a large number of journal and conference papers.

Prof. Nijmeijer was the Editor-in-Chief of the *Journal of Applied Mathematics* until 2009, a Corresponding Editor of the SIAM *Journal on Control and Optimization*, and a Board Member of the *International Journal of Control*, *Automatica*, *Journal of Dynamical Control Systems*, *International Journal of Bifurcation and Chaos*, *International Journal of Robust and Nonlinear Control*, *Journal of Nonlinear Dynamics*, and the *Journal of Applied Mathematics and Computer Science*. He was a recipient of the IET Heaviside Premium awarded in 1990. In the 2008 research evaluation of the Dutch Mechanical Engineering Departments, the Dynamics and Control Group was evaluated as excellent with regard to all aspects (quality, productivity, relevance, and viability).